

# Three-dimensional holographic fluorescence microscopy

**Bradley W. Schilling and Ting-Chung Poon**

*Bradley Department of Electrical Engineering, Virginia Polytechnic Institute and State University, Blacksburg, Virginia 24061*

**Guy Indebetouw**

*Department of Physics, Virginia Polytechnic Institute and State University, Blacksburg, Virginia 24061*

**Brian Storrie**

*Department of Biochemistry, Virginia Polytechnic Institute and State University, Blacksburg, Virginia 24061*

**K. Shinoda and Y. Suzuki**

*Central Research Laboratory, Hamamatsu Photonics K. K., 5000 Hirakuchi, Hamakita City 434, Japan*

**Ming Hsien Wu**

*Hamamatsu Corporation, Bridgewater, New Jersey 08807*

Received May 8, 1997

Most commonly used methods for three-dimensional (3D) fluorescence microscopy make use of sectioning techniques that require that the object be physically scanned in a series of two-dimensional (2D) sections along the  $z$  axis. The main drawback in these approaches is the need for these sequential 2D scans. An alternative approach to fluorescence imaging in three dimensions has been developed that is based on optical scanning holography. This novel approach requires only a 2D scan to record 3D information. Holograms of 15- $\mu\text{m}$  fluorescent latex beads with longitudinal separation of  $\sim 2$  mm have been recorded and reconstructed. To our knowledge, this is the first time holograms of fluorescent specimens have been recorded by an optical holographic technique. © 1997 Optical Society of America

In recent years three-dimensional (3D) imaging techniques such as laser scanning and confocal microscopy have been applied to fluorescence microscopy.<sup>1-4</sup> Although very successful, many of these 3D microscopy techniques involve sectioning and reconstitution. The approach used is to take a series of sections through the sample at different depths, image them, and then merge the information into a single 3D image. The required multiple two-dimensional (2D) scans needed to collect the 3D information is the major drawback of these methods. The 3D scanning process is time consuming and requires a precise mechanical 3D positioning device. In cases in which photobleaching is a concern, repeated 2D sectioning only exacerbates this problem by increasing exposure.

An attractive quality of holography is the inherent ability to store 3D information in a 2D array without a depth scan. Elimination of the 3D scanning process gave us the impetus to investigate holographic techniques for fluorescence microscopy. A novel approach to 3D imaging has been developed based on optical scanning holography<sup>5</sup> (OSH). We propose a new type of microscope that combines the 3D imaging capability of OSH with the advantages of fluorescence techniques. This research, which brings these ideas together for the first time to our knowledge, will lead to the first 3D fluorescence holographic microscope. We defer all theoretical and background discussion of OSH to the published literature.<sup>5-8</sup> A detailed treatment of this topic is being submitted for publication.

Another important aspect of the OSH method is the incoherent nature of the technique. An essential aspect of holographic recording is that each object point creates a Fresnel-zone pattern (FZP) on the recording media.<sup>9</sup> This is accomplished by the FZP scanning technique employed in OSH, resulting in a hologram that contains information of only the object intensity variations and is insensitive to its phase variations. This feature is essential since it allows the holographic recording of not only absorbing or scattering objects but also fluorescent objects. Also noteworthy is the fact that in OSH the bias as well as the twin image can be conveniently removed by electronic and (or) digital means.<sup>10</sup> This contrasts with other incoherent holographic techniques that are plagued by a rapid bias buildup when the object consists of more than a few point scatterers.<sup>11</sup>

OSH is based on scanning the object with a temporally modulated FZP. The FZP is generated by superimposing a plane wave with a spherical wave from the same laser. The 3D location of the scatterer is encoded in the position and size of the FZP.<sup>9</sup> For heterodyne detection, the FZP is temporally modulated by interfering two waves of different temporal frequencies that are adjusted by an acousto-optic device. To apply OSH to fluorescent specimens, we generate the FZP at a wavelength near the peak absorption of the specimen. The simplified block diagram of our experimental setup in Fig. 1 shows two plane waves separated in frequency by  $\Delta\Omega$ . These plane waves

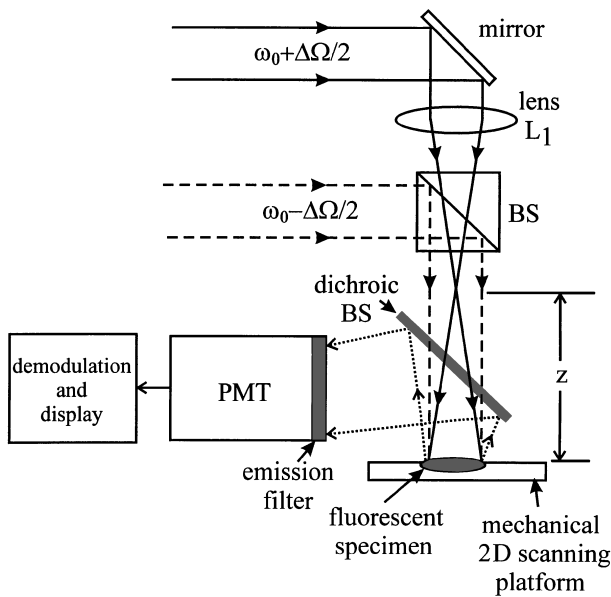


Fig. 1. Block diagram of the experimental setup used to record the hologram of a fluorescent specimen by optical scanning holography. BS's, beam splitters; PMT, photomultiplier tube.

originate from the 514-nm line of a multiline argon-ion laser ( $\omega_0 = 2\pi c/\lambda = 3.667 \times 10^{15}$  rad/s). The frequency shift in each beam is achieved by an acousto-optic modulator (AOM). The AOM is used in a configuration that splits the laser light into two beams separated in frequency by  $\Delta\Omega = 2\pi \times 10.7$  MHz. The beams are then collimated and made parallel to each other as shown in the figure. A lens is placed in one of the beams to form the spherical wave, which is then combined collinearly with the other beam at the beam splitter. The resulting interference pattern at the object, which is a distance  $z$  beyond the focus of the spherical wave, is the FZP laser field. The dichroic beam splitter ( $T = 514$  nm,  $R = 595$  nm) allows light at 514 nm to pass and excite the fluorescent object, which fluoresces strongly at the center frequency of 560 nm. This light is reflected by the dichroic beam splitter and passes through a 595-nm narrow-bandpass filter (used to reject the background laser light at 514 nm) and into the photomultiplier tube. The object is scanned through the FZP in a raster pattern by a computer-controlled mechanical  $x$ - $y$  scanning platform. The PMT current, which contains 3D information of the object being scanned, is electronically filtered and amplified at 10.7 MHz and demodulated and digitized by a standard PC-based analog-digital board. This digitized intensity pattern is stored in a 2D array in accordance with the scanning to produce the hologram.

The fluorescent sample used in the experiment was a solution containing a high concentration of fluorescent latex beads. The beads were 15  $\mu\text{m}$  in diameter with peak excitation at 530 nm and peak emission at 560 nm. These beads made good experimental specimens because they have a quantum efficiency near 100%, broad excitation and emission bands, and a fluorescent lifetime shorter than 10 ns.<sup>12</sup> To demonstrate

the depth-discriminating capability of the system, we used a fluorescent object that consisted of two wires placed next to each other parallel to the optical axis but with their ends at slightly different distances from the focus of lens  $L_1$ . A drop of fluorescent solution was placed on the end of each of these wires. A hologram of this fluorescent sample was recorded and is shown in Fig. 2. The two drops, easily distinguishable in the hologram, are separated in depth by approximately 2 mm, with the drop on the left at  $z_0 \approx 35$  mm and the drop on the right at  $z_1 \approx 37$  mm. The area scanned to produce the hologram is approximately 2 mm  $\times$  2 mm. The hologram is a 256 by 256 array with intensity level represented by 256 gray levels.

Once the hologram (Fig. 2) has been recorded and stored, the 3D image can be reconstructed either optically or numerically. Numerical image reconstruction is based on convolving the hologram with the free-space impulse response corresponding to the desired depth  $z$ . Once again we emphasize the difference between the holographic technique and standard 3D imaging techniques. In optical sectioning methods the image is brought into focus at a chosen depth, say  $z_0$ , and the 2D image for that plane is recorded and stored. This process is repeated for as many planes in  $z$  as desired, and an image must be recorded and stored for each plane. With OSH, a hologram of the object is recorded and stored with a single 2D scan. Since all the depth information is stored in the hologram, any desired image plane can be brought into focus during image reconstruction. Numerical image reconstruction has been performed on the hologram shown in Fig. 2 for two different depths. Figure 3 is a reconstructed image at  $z_0 = 34.5$  mm, and Fig. 4 is an image reconstruction at  $z_1 = 36.8$  mm. Since the individual attributes in each fluorescent drop are not obvious in Figs. 3 and 4, arrows have been overlaid on the figures to point out certain areas of interest. In Fig. 3 the fluorescent drop on the left is in better focus than that

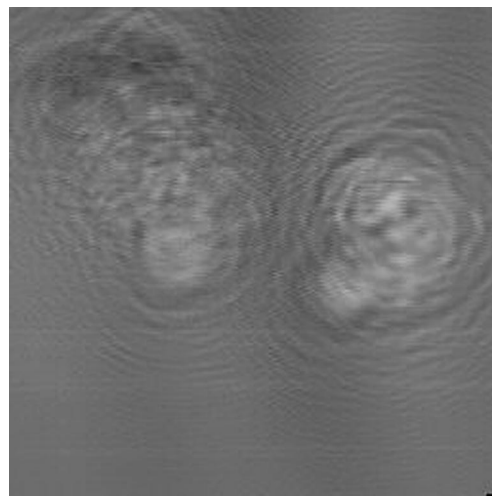


Fig. 2. Hologram of a fluorescent specimen recorded by OSH. The object consists of two drops of solution containing a high concentration of fluorescent latex beads separated in depth by  $\sim 2$  mm. The image is a 256-level gray-scale image consisting of 256 by 256 pixels. The area scanned is approximately 2.0 mm  $\times$  2.0 mm.

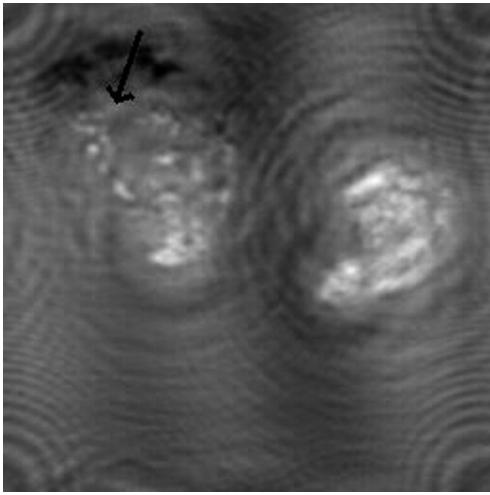


Fig. 3. Reconstruction of the hologram shown in Fig. 2 at a depth of  $z_0 = 34.5$  mm. The arrow shows individual fluorescent beads that are in focus at this depth.

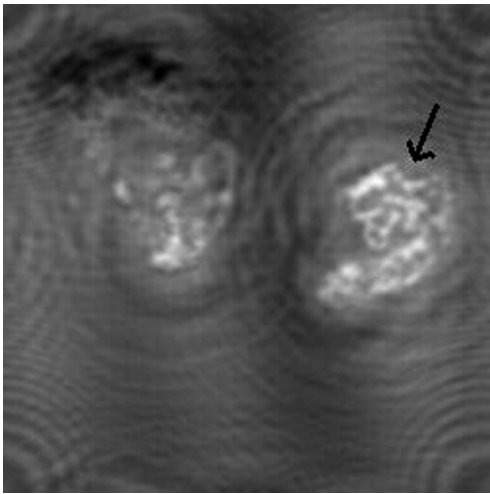


Fig. 4. Reconstruction of the hologram shown in Fig. 2 at a depth of  $z_1 = 36.8$  mm. The arrow shows four individual fluorescent beads that are in focus at this depth.

on the right. The arrow in Fig. 3 points to particular beads that are better imaged when the hologram is reconstructed at depth  $z_0$  than in Fig. 4 at depth  $z_1$ . Similarly, the arrow in Fig. 4 points out a string of four beads that can be individually distinguished when the hologram is reconstructed at depth  $z_1$  but that are blurred in the image-reconstruction plane  $z_0$  in Fig. 3. No attempt was made to eliminate the twin image in these reconstructions, which explains the residual fringing that was observable in these images.

One reason that the differences between Figs. 3 and 4 are not more striking lies in the limited resolving power of the optics used in our experiment. The resolution of the OSH system is limited by the system's numerical aperture (NA), which in turn depends on the focal length of lens  $L_1$  of 150 mm and the diameter of the plane wave focused by lens  $L_1$  ( $D = 10$  mm). The diffraction-limited resolution limits for our system can be calculated from the following equations<sup>13</sup>: lateral resolution,  $\Delta x = \lambda/2NA$ ; longitudinal resolution,  $\Delta z =$

$\lambda/NA^2$ , where  $\lambda$  is the wavelength of the laser. The NA of our system is approximately 0.033, which corresponds to diffraction-limited resolution limits of  $\Delta x = 7.7 \mu\text{m}$  and  $\Delta z = 200 \mu\text{m}$ . The 15- $\mu\text{m}$  bead size is very close to the limit that we can expect to resolve laterally with our current setup and more than an order of magnitude beyond what we can resolve in the  $z$  dimension. At this proof-of-principle stage, our optics have not been optimized for resolution. When imaging takes place in the air, the practical limit for NA is  $\sim 0.95$ . Assuming that the setup could be optimized to achieve such a NA the theoretical limits of resolution for 3D holographic fluorescence microscopy by this method are  $\Delta x = 0.3 \mu\text{m}$  and  $\Delta z = 0.6 \mu\text{m}$ .

We have presented a novel approach to 3D fluorescence microscopy based on optical scanning holography. The holographic technique has a number of advantages over current 3D sectioning methods. These advantages stem from the fact that 3D information can be recorded holographically with a single 2D scan. A hologram of fluorescent beads has been recorded and numerically reconstructed at different depths, demonstrating the ability of this technique to record depth information. To our knowledge, this is the first time a hologram of a fluorescent specimen has been recorded by an optical holographic technique. Further optimization will bring the resolution capability of the system closer to the theoretical limits of  $\Delta x = 0.3 \mu\text{m}$  and  $\Delta z = 0.6 \mu\text{m}$ .

B. Schilling thanks Brian Redman for his insightful comments and suggestions. Special thanks to Jonathan Lei and James Habersat for their contribution. This study has been supported by National Science Foundation grants under the Directorate of Biological Sciences (BIR-9419342) and the Directorate of Engineering (ECS-9319211).

## References

1. J. S. Ploem, *Appl. Opt.* **26**, 3226 (1987).
2. D. J. Arndt-Jovin, M. Robert-Nicoud, S. J. Kaufman, and T. M. Jovin, *Science* **230**, 247 (1985).
3. S. Hell and E. H. K. Stelzer, *J. Opt. Soc. Am. A* **9**, 2159 (1992).
4. S. Kimura and C. Munakata, *Appl. Opt.* **29**, 489 (1990).
5. T.-C. Poon, M. H. Wu, K. Shinoda, and Y. Suzuki, *Proc. IEEE* **84**, 753 (1996).
6. T.-C. Poon and A. Korpel, *Opt. Lett.* **4**, 317 (1979).
7. T.-C. Poon, *J. Opt. Soc. Am. A* **2**, 521 (1985).
8. T.-C. Poon, K. B. Doh, B. W. Schilling, M. H. Wu, K. Shinoda, and Y. Suzuki, *Opt. Eng.* **34**, 1338 (1995).
9. L. Mertz and N. O. Young, *Proceedings of the Conference on Optical Instruments and Techniques*, K. J. Hall, ed. (Chapman & Hall, London, 1962), pp. 305–317.
10. K. Doh, T.-C. Poon, M. H. Wu, K. Shinoda, and Y. Suzuki, *Opt. Laser Technol.* **28**, 135 (1996).
11. A. Kozma and N. Massey, *Appl. Opt.* **8**, 393 (1969).
12. R. P. Haugland, *Handbook of Fluorescent Probes and Research Chemicals*, 5th ed. (Molecular Probes, Inc., Eugene, Ore., 1992).
13. P. C. Cheng, T. H. Lin, W. L. Wu, and J. L. Wu, *Multidimensional Microscopy* (Springer-Verlag, New York, 1994).